

Line Drawing Guided Progressive Inpainting of Mural Damages

Luxi Li, Qin Zou, Fan Zhang, Hongkai Yu, Long Chen, Chengfang Song,
Xianfeng Huang, Xiaoguang Wang

Abstract—Mural image inpainting refers to repairing the damage or missing areas in a mural image to restore the visual appearance. Most existing image-inpainting methods tend to take a target image as the only input and directly repair the damage to generate a visually plausible result. These methods obtain high performance in restoration or completion of some specific objects, e.g., human face, fabric texture, and printed texts, etc., however, are not suitable for repairing murals with varied subjects, especially for murals with large damaged areas. Moreover, due to the discrete colors in paints, mural inpainting may suffer from apparent color bias as compared to natural image inpainting. To this end, in this paper, we propose a line drawing guided progressive mural inpainting method. It divides the inpainting process into two steps: structure reconstruction and color correction, executed by a structure reconstruction network (SRN) and a color correction network (CCN), respectively. In the structure reconstruction, line drawings are used by SRN as a guarantee for large-scale content authenticity and structural stability. In the color correction, CCN operates a local color adjustment for missing pixels which reduces the negative effects of color bias and edge jumping. The proposed approach is evaluated against the current state-of-the-art image inpainting methods. Qualitative and quantitative results demonstrate the superiority of the proposed method in mural image inpainting. The codes and data are available at <https://github.com/qinnzou/mural-image-inpainting>.

Index Terms—Mural inpainting, cultural heritage preservation, mural image dataset, image inpainting, histogram loss

I. INTRODUCTION

AS one of the most cherished world cultural heritages, murals in Dunhuang Mogao Grottoes represent more than one thousand years of Chinese history and culture from the late Jin Dynasty to the early Song Dynasty. In this long history, due to the natural weathering and human damage, Mogao Grottoes suffered from the cracking, color fading, and many other forms of distresses, which gradually destroyed the murals. The traditional mural restoration method is inclined to paint on the cultural relics directly, making the restoration

L. Li, F. Zhang, X. Huang are with the State Key Laboratory of Surveying, Mapping, and Remote Sensing Information Engineering, Wuhan University, Wuhan 430079, China (e-mails: lucylee@whu.edu.cn, zhangfan@whu.edu.cn, huangxf@whu.edu.cn).

Q. Zou and C. Song are with the School of Computer Science, Wuhan University, Wuhan 430072, China (e-mails: qzou@whu.edu.cn, songchf@whu.edu.cn).

H. Yu is with the Department of Electrical Engineering and Computer Science, Cleveland State University, OH 44115, USA (E-mail: hongkaiyu2012@gmail.com).

L. Chen is with the Institute of Automation, Chinese Academy of Sciences, Beijing 100190, China (e-mail: long.chen@ia.ac.cn).

X. Wang is with the School of Information Management, Wuhan University, Wuhan 430072, China (e-mail: wxguang@whu.edu.cn).

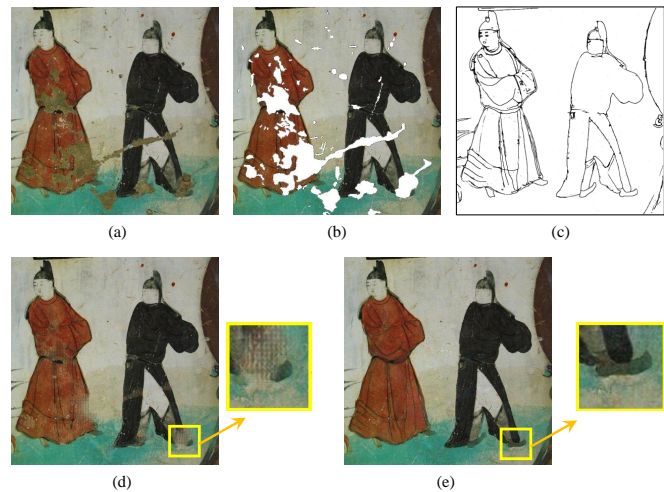


Fig. 1. Inpainting with and without the assistance of line drawings. (a) An image of damaged mural. (b) The mask for inpainting. (c) The corresponding line drawings of the mural. (d) The inpainting results without line drawings. (e) The inpainting result with line drawings.

result irreversible, which may cause secondary damage to the murals. While digitization technologies allow permanent digital storage of the original shape and appearance, the digital inpainting of murals is of great significance to the protection of cultural heritage.

Over the past decade, a number of advanced inpainting methods built on deep convolutional neural networks (DCNN) have been proposed [1]–[6]. These methods perform well on natural image inpainting, and achieve outstanding results on the public available datasets such as CelebA [7], Places2 [8], and ParisStreetView [9]. However, they meet some problems when applied to mural images. First, the missing parts of the mural may be large and complex, which are difficult to recover directly from the mural images. In mural inpainting, an important requirement is that the murals are restored to the original appearance as much as possible. However, traditional inpainting strategies using only the damaged mural image as input may generate results that do not match the truth, although the results may be visually plausible, as illustrated by Fig. 1. Second, even with the assistance of line drawings, existing DCNN-based inpainting methods may still suffer from color bias. In most cases, pixels of the whole image are involved in the convolution-pooling computation, where position bias of pixels may be introduced in the downsampling and upsampling procedures. Meanwhile, the color difference will be apparent

when we merge the generation part in the mask and the known part outside the mask as a lack of color-consistency control in most DCNN-based methods, as illustrated by Fig. 2.

Although existing methods are not completely suitable for mural inpainting, they do provide us inspirations. The idea of ‘line first, color next’ proposed in [10] predicts the structure lines first, and then combines the lines for structure restoration. It proves that edge maps contribute to structure-aware inpainting. In mural inpainting, the restored images are expected to be consistent with the original murals as much as possible. Considering that edge maps of the mural structure predicted by neural networks are not up to the expert level, we adopt the line drawings manually produced by professional painters as the guidance in the inpainting task. In [11], a coarse-to-fine inpainting strategy was put forward, which divides the inpainting process into two stages. It first restores to get a rough low-quality result, and then refines the result to obtain a high-quality final result. Inspired by this ‘task disassembly’ idea, we divide our mural inpainting task into two sub-tasks. Accordingly, we complete these sub-tasks in two separated stages, namely structure reconstruction and color correction.

In view of the problems of mural inpainting mentioned above and the inspiration from existing methods, we propose a progressive mural inpainting method guided by line drawings. Note that, it is a two-stage inpainting method. In this method, we not only pay attention to the inpainting strategies, but also give much consideration to the particularity of murals. Specifically, first, we introduce line drawings of the damaged mural in the first stage. As line structures can basically determine the content of the mural paintings, we input the line drawings into the network, which we expect to drive the network to generate results as close as possible to the real murals. In this way, we will solve the problem of low authenticity of inpainting of large damaged area. Second, we employ the histogram loss [12] in the second inpainting stage, which is the first time in use to ameliorate the texture-blur and color-bias problem in an image-inpainting task.

In the implementation of the above idea, we divided the inpainting into structural fusion and color adjustment. Different from other methods which introduce structure lines and handle structures and colors together [2], [4], [10], we consider the structure and the color separately. The damaged structure is rebuilt in the first inpainting stage, which ignores the color difference. While in the second inpainting stage, the color of the image is adjusted with the completed structures, which would optimize the overall sense, and largely ameliorate the color difference problem. Qualitative and quantitative evaluations are conducted by comparing the proposed method with the current state-of-the-art image inpainting methods.

The contributions of this work are summarized as follows:

- First, to the problem of large-area mural damage inpainting, we introduce the line drawing as an assistance and the histogram loss as a constraint in the inpainting, which greatly improves the inpainting quality on damaged mural with large holes.
- Second, to the problem of color bias in mural inpainting, we propose a novel inpainting strategy that decomposes the inpainting into two subtasks – structure reconstruction



Fig. 2. Color-bias problem in image inpainting. Top row: mural images with masks in white. Bottom row: the inpainting results.

and color correction, which not only restores the structure, but also keeps the color consistent.

- Third, we construct a mural image dataset consisting of 1,714 mural paintings from Dunhuang Mogao Grottoes. Each mural image has a corresponding line drawing. The dataset has been released to the community, which would promote the research of mural inpainting and heritage preservation.

II. RELATED WORK

A. Image Inpainting

Image inpainting has been a hot research topic in the field of computer vision and image processing [13], [14]. Over the past few years, a number of excellent image inpainting methods built on deep learning techniques have been developed. In these methods, some used the strategy of structure-information embedding. For example, Nazeri [10] put forward the idea of ‘line first, color next’, and conducted the inpainting separately for line drawing and color, which is considered as a SOTA method and has been widely compared by other works. In [15], a novel visual structure reconstruction (VSR) layer was designed to entangle reconstructions of the visual structure and visual feature, which benefits each other by sharing parameters. In [16], the manga inpainting task was divided into structural line inpainting and screen VAE map inpainting, which learned the semantic difference between structure and screentone. In [17], a mutual encoder-decoder CNN was proposed for joint recovering of both structures and textures in two branches, which effectively removes the blur and artifacts caused by inconsistent structure and texture features. In [18], the structure information was applied to inpainting of medical images, with significantly improved performance.

The coarse-to-fine inpainting strategy is also widely used. In [11], in the first stage the network generates a coarse result with low resolution. While in the section stage, the previous

result is enhanced with a refine network, where global and local images are input to the discriminator respectively to get global critics and local critics. This approach generates results look fine in both global and local view, but limits its masks to be rectangular, which is inapplicable to regions with irregular shapes. In [19], a two-stage network was proposed that uses a coherent semantic attention layer to preserve the spatial structure of the image within the refinement network. In [20], dynamic-to-static image translation is delicately formulated as an image inpainting problem, and a novel coarse-to-fine framework is proposed. In [21], a decoding network was adopted with coarse and inpainting paths, and the number of convolution operations was reduced by sharing the coarse weight with the inpainting paths.

With the success of partial convolution [1], which can ablate the mask layer by layer to make full use of known information and transmit background information into the holes, some methods have been built on partial convolution for image inpainting. In [15], a P-UNet was introduced as the backbone, which replaces each convolution layer in U-Net with a partial convolution layer, in order to capture the local information of irregular boundaries. In [22], partial convolution is adopted to avoid the interference of mask areas on generated results. In [4], the gated convolution was introduced to improve the mask mechanism of partial convolution from rule-based mask to learning-based mask, and reduce the limitation of rectangular mask in their former work [11].

The attention mechanism is well studied in image inpainting. In [23], a U-NET architecture was exploited that used a cross-layer attention and pyramid filling mechanism. The encoder learned region affinity by attention from a high-level semantic feature map, and transferred the learned attention to its adjacent high-resolution feature map. In [22], a multistage attention module was introduced to ensure better results in multi-scale. In [24], a spatial similarity-based attention mechanism was proposed to guarantee the local intra-level continuity. In [25], a novel dual attention fusion module was proposed to explore feature interdependencies in spatial and channel dimensions and blend features in missing regions and known regions. It found that the smooth contents with rich texture information can be naturally synthesized.

Semantic information has been increasingly considered in image inpainting in recent years. In [26], a new cross semantic attention layer was introduced to exploit the long-range dependencies between the known parts and the completed parts, which can improve realism and appearance consistency of repaired samples. In [27], a novel deep generative model was proposed. It equipped with a style extractor that can extract the style feature (latent vector) from the ground truth. The model can generate a large number of results consistent with the context semantics of the image. In [28], an end-to-end framework named progressive generative networks (PGN) was proposed, which regards the semantic image inpainting task as a curriculum learning problem. In [29], a Semantic-Wise Attention Propagation (SWAP) module was developed to refine the restored image textures across scales by exploring non-local semantic coherence, which effectively mitigates the mix-up of textures.

B. Mural Inpainting

Mural image inpainting is a branch of image inpainting, which has attracted more and more attention in recent years [30], [31]. At first, image inpainting methods are adopted to restore mural images. In [32], a semi-automatic scratch detection method was proposed for mural damage localization, based on which the pixel filling and color restoration was performed by different variational inpainting methods. With the success of deep learning techniques in visual tasks, researchers started to apply deep learning-based techniques to handle the mural inpainting problem. In [33], an auto-encoder generative adversarial network (AGAN) was proposed, which achieved much better performance over the traditional methods.

Some methods considered the importance of structure for murals. In [34], a structure-guided mural inpainting methods built on EdgeConnet [10] obtained good results in mural restoration. In [35], line drawings were used to guide the mural inpainting under a sparse-representation framework. In this method, the results obtained are more realistic and are closer to the original mural paintings than that of the conventional methods.

Some methods realized the importance of fidelity in mural inpainting. In [36], a 2-phase original-restoration-driven learning method was proposed to guide the model to restore the original content of the Thanka mural. In [37], a JPGNet was proposed to combine the advantages of predictive filtering and generative network, which can preserve local structures while removing the artifacts and filling the numerous missing pixels, based on the understanding of the whole scene.

Some methods took the partial convolution in their networks to get better performance. In [38], partial convolutions assisted with the sliding window were employed for mural inpainting. However, the relation of structure retention and color restoration in this method was not well resolved yet. In [39], a Thanka mural inpainting method was proposed based on multi-scale adaptive partial convolution. On the stroke-like damages, this method obtains results that are relatively close to the real value. While on heavily damaged regions with complex textures, it still has limitations and difficulties in achieving visual plausible results.

In summary, existing mural inpainting methods still have various problems. A lot of room has been left for improvement.

III. METHODOLOGY

In this section, we first introduce the system overview and the network design, and then describe the self-attention module and loss functions of the proposed neural network.

A. Overview

Figure 3 illustrates our approach. Given a mask image, we combine it with the corresponding line drawing as the input of the structure reconstruction generator (G1). Then, it fills the missing regions, and the generated image is concatenated with the irregular mask as the input of the color correction generator (G2), which will evaluate the residual adjustments to reduce the color difference. Finally, the inpainted image is obtained, where the pixels in the missing regions are adjusted

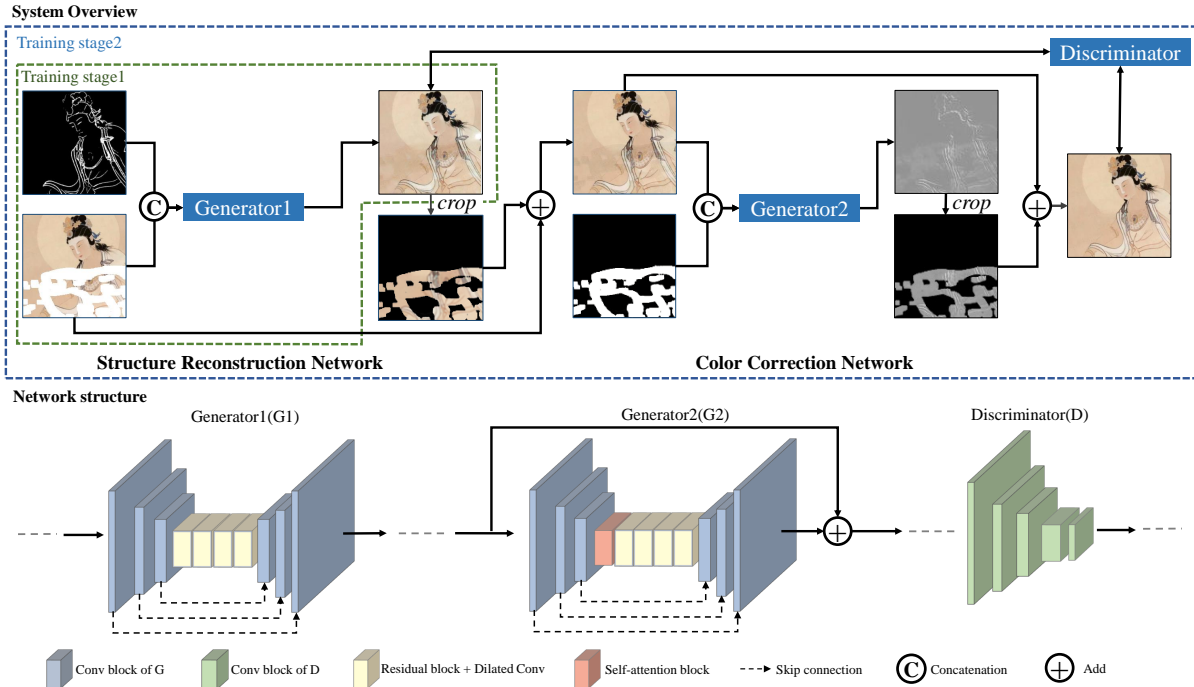


Fig. 3. The system overview and network structure of the proposed network. The upper part illustrates the system overview, the lower part illustrates the details of network structure. The whole model is composed of a Structure Reconstruction Network (SRN) and a Color Correction Network (CCN). SRN generates an approximate result with a complete structure, which is input into the CCN to generate a color-consistent final result.

appropriately while the outside pixels restored to the proper values.

The input of our network model includes a mural image, a line drawing, and a mask. The mask indicates the missing region to be recovered. In the first stage, we generate an overall well-structured result by the structure reconstruction network (SRN), and then rectify the local hole-region by the color correction network (CCN) in the second stage. Therefore, the masked image and line drawing are the input to SRN, and the mask channel is the input to CCN.

Our inpainting method works from global to local. In SRN, the image generated by G1 directly participates in loss calculation, getting all the pixels backward so that the network is trained to generate globally reasonable results. In CCN, a four-channel image combined by the outcome image of G1 and a mask channel, is fed into G2 to evaluate the residual adjustments, which applied to the missing regions only. The final image combined of the to-be-recovered regions and the background of the original input image, is differentiated by discriminator loss and color correction loss functions to refine the local results.

Accordingly, the training is also divided into two stages. In training stage 1, SRN is trained separately. The training stage 2 does not start until G1 and D come up to converge. Since D has already learned to distinguish the ground truth and the initial generated results, G2 will converge quickly under the guidance of D.

B. Network Architecture

Structure Reconstruction Network (SRN) In the structure reconstruction network, we concatenate the damaged mural

painting with the corresponding edge map as the input to G1. The network has an encoder-decoder architecture [40]. Firstly, through three down-sampling convolutions, the size of the image shrinks to one-eighth of the initial. Then there follow three up-sampling convolutions and four residual blocks. We apply instance normalization [41] across all layers of the network. We apply skip layers connecting every up-sampled layer with the former corresponding down-sampled layer. Skip layers give the generator a way to circumvent the down-sample bottleneck for information [42]. Specifically, these skip layers convey low-level multi-scale details for the last few layers to be restored to the original resolution. Moreover, initial color information gets constantly emphasized through skip layers such that the color difference would be enforced to the greatest extent.

Color Correction Network (CCN) Color correction network (CCN) takes the concatenation of the image and its mask as input, the backbone architecture of CCN keeps the same with SRN. CCN takes a global residual strategy, meaning that the input mural painting of G2 is added to the output of G2, the task of CCN boils down to evaluate the residual values of the structure-reconstructed image. We found the global residual contribute a lot to the inpainting effect in our network, as the image has already been well-restored through SRN and what CNN need to do is slightly adjust the missing-region pixels instead of modifying the entire image. Moreover, a self-attention mechanism is employed in CCN, which estimates the scores of attention at each pixel. The attention mechanism extends the receptive field to global and exploits the high similarity area to adjust pixel values. Therefore, for blocks

with repetitive structure, the network can restore the color consistent with other blocks.

Discriminator Due to the different training purposes of the two stages, existing two-phase GANs tend to install distinct discriminators for the two generators respectively [10], [43], or just follow the second generator [3], [4]. However, in our network model, both generators share a single discriminator. Although the aims of two networks are different: the former focuses on the integration of the whole structure while the latter focuses on local color difference adjustment, the final training purpose is still the same, that is, to generate images identical to the ground truth. Thus, both generators connect with the same discriminator in our network.

For discriminators, we use the same 70×70 PatchGAN [4], [10] architecture as in [10]. The 70×70 PatchGAN determines whether or not overlapping image patches of size 70×70 are real. Each green conv block constitute discriminator in Fig. 3 includes a convolution operation, a spectral normalization [44] and a leakyRelu activation [45].

C. Self-Attention Module

In CCN, non-local proposed in [46] is employed. As convolutional operation processes a local neighborhood, either in space or time domain, long-range dependencies can only be captured when these operations are carried out repeatedly, which is computationally inefficient. The non-local operation does not confine to the local neighborhood but computes the response at a position as a weighted sum of the features at all positions in the input feature maps. In CCN, all the known pixels are calculated to optimize the color of pixels inside the hole. For images with large missing area, deep-inside-hole regions require to establish connections with the outside to adjust color, so non-local operation is adopted in our work.

The non-local operation is defined as:

$$\mathbf{y}_i = \frac{1}{C(\mathbf{x})} \sum_{\forall j} f(\mathbf{x}_i, \mathbf{x}_j) g(\mathbf{x}_j), \quad (1)$$

where i is the index of an output position whose response is to be computed and j is the index that enumerates all possible positions. x is the input image, and y is the output image holding the same size as x . f indicates similarity between position i and position j in x , and g represents the pixel value at the position j . The response is normalized by a factor $C(\mathbf{x})$. Embedded Gaussian is used as f function, formulated as $f(\mathbf{x}_i, \mathbf{y}_i) = e^{\theta(\mathbf{x}_i)^T \phi(\mathbf{x}_j)}$. Given $C(\mathbf{x}) = \sum_{\forall j} f(\mathbf{x}_i, \mathbf{y}_i)$, then we get

$$\mathbf{y}_i = \text{softmax}(\theta(\mathbf{x}_i)^T \phi(\mathbf{x}_j)) g(\mathbf{x}_i), \quad (2)$$

where $g(x) = wx$, w is a learnable weight matrix. Specifically, it first projects the feature map x into two spaces, and computes the similarity between every two pixels by dot product, then calculates through a *softmax* activation function, and finally computes the attention map by dot product with $g(\mathbf{x})$.

D. Loss Functions

The loss function of GAN [47], consists of two parts: generator loss and discriminator loss. Discriminator loss measures

whether the discriminator's judgment is consistent with the truth. Adversarial loss in generator loss measures how close the generated picture is to the real one. In the game between these two loss functions, the resultant image will gradually come near to the ground truth.

In our network, the generator loss ($L_{Generator}$) is composed of the perceptual loss [48], L1 loss, and histogram loss [12], as defined by Eq. (3):

$$L_{Generator} = L_{Gram} + L_1 + L_{Histogram}. \quad (3)$$

The perceptual loss (L_{Gram}) aims for general image reconstruction, L1 loss (L_1) for color correction, and histogram loss ($L_{Histogram}$) for rectifying the color distribution while avoiding ambiguity. In the following, we introduce these losses in detail.

Perceptual Loss Perceptual Loss is proposed in style transfer [48], which is widely used in the field of style transfer and image repair in recent years. It contains style loss and content loss, as shown in Eq. (4),

$$L_{Gram} = \alpha L_{Content} + \beta L_{Style}. \quad (4)$$

Gram matrix can express pixel arrangement features to simulate image style. In mural inpainting, the color arrangement has obvious style characteristics, thus, we apply gram loss in the inpainting task so that the generated part has a similar color style as the known pixels, and make the overall vision be natural and reasonable.

The style loss is formulated by Eq. (5):

$$L_{Style} = \sum_{l=0}^L w_l \frac{1}{4N_l^2 M_l^2} \sum_{i,j} (G_{ij}^l - A_{ij}^l)^2, \quad (5)$$

where G^l and A^l are respectively the gram matrix of output image and target image at layer l . Nl is the number of different feature maps in layer l , and Ml is the volume of feature maps in layer l .

The content loss is formulated by Eq. (6):

$$L_{Content} = \frac{1}{2} \sum_{i,j} (F_{ij}^l - P_{ij}^l)^2, \quad (6)$$

where F^l and P^l are respectively the feature maps of the output image and reference image in layer l of the pre-trained VGG19 model, i and j denote the size of the feature map in layer l .

L1 Loss L1 Loss, namely Mean Absolute error (MAE) [48] is the sum of the absolute difference between the target value and the predicted value. L1 loss is used to measure the absolute distance between the inpainting result and the ground truth, we aim to reduce the distance as much as possible in the training. The L1 loss is formulated by Eq. (7):

$$MSE = \frac{\sum_{i=1}^n (y_i - y_i^p)^2}{n}, \quad (7)$$

where y is the pixel value of the ground truth and y^p is that of the predicted image.

Histogram loss Histogram loss [12] is proposed to solve the problem of instabilities in texture synthesis of Gatys [48]

method. Gram matrix tends to produce average results, making the results of texture mapping look fuzzy. However, the introduction of histogram loss can guide the pixel distribution of generated results to maintain original variance and standard deviation. In our experiment, we also noticed the problem of the average distribution of pixels caused by Gram matrix. Besides, as is known, L1 will incentivize an averaged grayish color when it is uncertain which color a pixel should take on, according to the research of Luan [49]. The combination of GAN network and L1 Loss can mitigate such problem. In our work, histogram loss is also adopted to more vigorously correct the color distribution range and solve the possible fuzzy problem attributed to Gram matrix. The histogram loss is formulated by Eq. (8):

$$L_{\text{histogram}} = \sum_{l=1}^L \gamma_l \|O_i - R(O_i)\|_F^l, \quad (8)$$

where O is output image, $R(O)$ is the histogram matching result of O and target image, γ_l is weight controlling the influence of layer l .

The loss functions described above are used at different training stages. As mentioned above, in the first training phase, we only train the structure reconstruction network. The aim of this stage is to generate a basic result from the line drawing and damaged image. As a rectified term, the histogram loss performs better with a preliminary result, and the time complexity and space complexity of the algorithm are both high. Therefore, under the comprehensive consideration, we don't employ the histogram loss in the first stage. In the second training phase, perceptual loss, L1 loss and histogram loss are used together for the two generators. Since color correction network focuses on local color adjustment, G2's loss function only calculates the loss in the missing regions.

IV. EXPERIMENTS AND RESULTS

In this section, we introduce the dataset used in the experiments, the training strategy, the comparison with the-state-of-the-art, and the results of ablation study.

A. Dataset

From Dunhuang Mogao Grottoes, due to the extensive damage of murals, there are not so many complete or well-preserved mural paintings available for training a deep neural model. In our research, we collect some replicas of murals by artists in addition to the real mural paintings. The real mural paintings are captured by digital cameras, while the replicas of murals are obtained by scanning the album. 1,714 images are collected. Among them, there are 525 real murals and 1,189 replicas. Through data augmentation operations such as rotation, random cropping, color transformation and flipping, a total of 75,072 images constitute our dataset. For masks, we adopt the public mask dataset released in [1].

Besides mural images, line drawings are also contained in our dataset. Lacking existing precisely corresponding line drawings, we resort to line-extracting methods to generate line drawings and ensure that there are no pixel offsets between

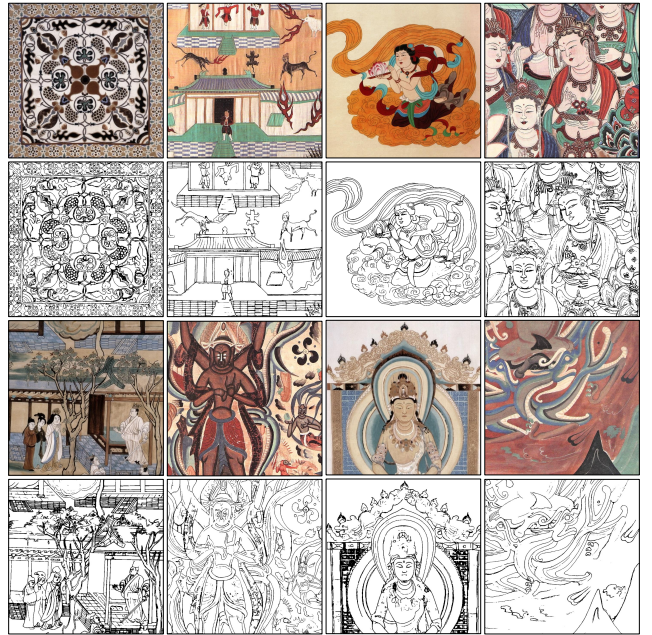


Fig. 4. Mural paintings and corresponding line drawings in our dataset.

line drawings and original images. Among these methods, we find the DexiNed [50] model can generate thin line maps that are plausible for human eyes, and it can be applied without pre-training or fine-tuning, which fits well our line-extracting task. We employ this method in our data preparation phase. Even though, noise is still unavoidable. In order to denoise to a large extent, we use the bilateral filter [51] to pre-process the mural image, which can reduce noise and smooth the image while maintaining the structure edges. After that, we extract line maps with the DexiNed model. Finally, a threshold is set to binarize the line maps. Figure 4 shows some of our final line maps. For real mural damages, the missing structures in the line maps are repaired with the help of professional painters.

B. Training Strategy

Since the training process is divided into two parts, it is inevitable to have cumulative error because the latter generator depends on the output of the former generator. In the early stage of training, the highly randomness of generating results steer the output to be far from the ground truth, then the latter generator takes the wrong images as input so that the final result is severely inaccurate. It is meaningless to train the second generator in the early stage. Therefore, we took a two-stage training strategy: In the first training phase, SRN gets trained separately. After 8 epochs of training, G1 and D come to converge, G1 starts to generate well-structured paintings, integrating the structure information in edge maps. Then, add CCN to the training in the second phase. On account of the discriminator being well-trained, G2 converges quickly under its guidance.

We implement our model with PyTorch 1.4.0 and Cuda 10.1. Our network is trained using the ADAM optimizer [53] with a total of 16 epochs on four NVIDIA GTX 2080 GPUs. The learning rate of D and G are set to 0.0001 and 0.00001



Fig. 5. Inpainting results of five mural images obtained by our method and three comparison ones - Deepfillv2 [4], EdgeConnect [10], and RFR [52]. Every two columns shows an inpainting example, the first line displays the damaged paintings and groundtruth, then the four results are listed in the next few lines in order of Ours, Deepfillv2, EdgeConnect and RFR. To illustrate clearly, the picture with blue borders magnifies the region enclosed by the left red box.

respectively, the epoch and batch size are set to 8, 32 in the first training stage and 8, 8 in the second training stage.

C. Comparisons with State-Of-The-Art Methods

In this subsection, qualitative and quantitative comparison is conducted between three state-of-art methods [4], [10], [52] with ours. In qualitative experiment, we analyze the advantages and disadvantages of each method. In quantitative experiment, we measure the results under several different metrics. Then, user study is conducted to prove our analysis of the experimental results. At last, we perform ablation experiment to verify the effectiveness of our network module design. All experiments are performed on our mural dataset.

We compare our method with three state-of-art methods, including DeepFillv2 [4], EdgeConnect [10] and RFR [52]. For fairness, we trained these models on our mural dataset. DeepFillv2 and EdgeConnect are trained with edges, while RFR is not able to be trained with edges due to its inpainting mechanism. These contrasted methods have the same characteristics as our methods in several different aspects. In Table I we compared them based on three dimensions: is or not a two-stage network, structure-guided, and have or not attention mechanism. All of these methods are trained with our dataset. We conducted qualitative analysis and quantitative analysis respectively to demonstrate the superiority of our method.

Qualitative Comparison. Figure 5 shows the comparison of our method and three state-of-the-art methods. We observe that EdgeConnect generates well-structured results owing to the involvement of line drawings, but shows severe color inconsistency between the hole and the background. RFR tends to produce checkerboard artifacts, and the structure can not be restored without the joint of line drawings. DeepFillv2 can restore relatively high-quality images with bright colors and

TABLE I
COMPARISON OF DIFFERENT APPROACHES INCLUDING DEEPFILLV2, EDGE CONNECT, RFR AND OUR APPROACH. THE COMPARISON OF IMAGE INPAINTING IS BASED ON THREE DIMENSIONS: MULTI-STAGE, STRUCTURE GUIDED, AND ATTENTION MECHANISM OPTION.

Method	Multi-Stage	LineGuided	Attention
DeepFillv2 [4]	✓	✓	✓
EdgeConnect [10]	×	✓	×
RFR [52]	×	×	✓
Ours	✓	✓	✓

TABLE II
QUANTITATIVE RESULTS OVER THE MURAL DATASET WITH MODELS: OURS, DEEPFILLV2 [4], EDGECONNECT [10] AND RFR [52]. THE BEST RESULT OF EACH ROW IS BOLD FACED.

Method	Ours	DeepFillv2	EdgeConnect	RFR
SSIM	0.8402	0.8269	0.8162	0.6881
MSE	0.0046	0.0055	0.0056	0.0108
PSNR	24.4421	23.719	23.3491	20.4586
LPIPS	0.1023	0.1131	0.1210	0.2537

clear textures, but it lacks the comprehensive consideration of overall colors. In comparison, our method achieves complete structure, clear detail and overall consistent colors.

Quantitative Comparison. Several metrics are adopted to illustrate the difference between these methods. we take MSE [54] SSIM [55], PSNR [56] and LPIPS [57] as evaluation metrics on our validation images, that is, MSE measuring pixel difference, SSIM measuring structure similarity, PSNR denoting the quality of images, and LPIPS evaluating image similarity that approximates human perception [58]. These metrics are calculated over 100 images of our mural validation set. Each image is assigned an irregular mask randomly. As shown in Table II, our method produces excellent re-

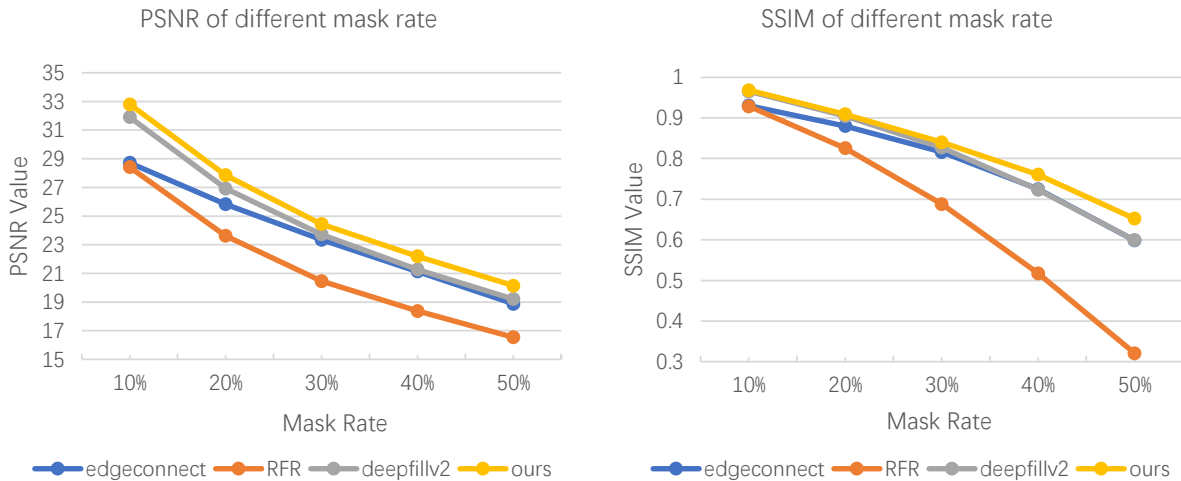


Fig. 6. Line charts of PSNR and SSIM in different ratio of masks. The left chart shows PSNR values of the four methods in different ratio of masks, the right shows SSIM values of them.

sults with the highest SSIM, PSNR, LPIPS, and the lowest MSE. Furthermore, we compared the inpainting effect of the four methods on different ratios of masks, respectively 10%, 20%, 30%, 40%, 50%. After calculating all the PSNR and SSIM values of the methods, we made a line chart as shown in Fig.6, in which our method excels others in both PSNR and SSIM in all ratios of masks. Deepfillv2 and RFR show a steady gap with our method in PSNR, EdgeConnect performs relatively better in ratio from 20% to 40%, but still not as good as Deepfillv2 and ours, while in SSIM, the gap between other method and ours become bigger and bigger as the ratio increases, especially RFR due to the lack of line drawings; Deepfillv2 is extremely close with ours when the mask ratio is low, but as the ratio goes upward, the gap tends to become bigger.

D. Experiment on real damaged murals

In the previous part, we conducted training and testing on our mural dataset. In order to verify the generality of our method, we conduct test experiment on the real damage murals. We mark the damaged area and complete the line drawing of the damaged image manually, then input the data into the network to inpaint the real damaged mural. Figure 7 shows the restoration effect of six groups of real murals. The first row shows the damaged murals, the second row shows the damaged areas with white masks, the third row shows the corresponding line drawings, and the fourth to seventh rows show the inpainting results of the proposed method, Deepfillv2, RFR, and EdgeConnect, respectively.

It can be seen from Fig. 7, the inpainting results combined with the structural information in the line drawing have completed the damaged area of the original mural and restored the mural style consistent with the original. The original tone is maintained, and the overall harmony and consistency as well as the clarity and integrity of the part are well kept.

E. User Study

We have performed a user study towards the inpainting result of the four methods. We randomly selected 10 images from the evaluation set, listed four different restored results with these methods for each image, and asked 10 users to rate the quality of them. Users scored them on a scale of 1 to 10 referring to the original paintings we provide. As a result, our methods got an average score of 8.42, while the scores of Deepfillv2, EdgeConnect, and RFR are respectively 7.6, 6.31, and 3.93. In Fig. 8, the four statistical charts from (a) to (d) show the user-evaluation results of the four methods, respectively. We sorted users' scores from high to low into four levels. The higher the score, the higher the level and the darker the color. The result confirms our analysis that our approach outperforms EdgeConnect and RFR, but the results of Deepfillv2 and ours are close in some cases. We find that Deepfillv2 has already done well in image inpainting, whose results are brightly colored and clearly textured. However, in terms of whole harmony, our approach is more holistic, which is very important for the murals with distinctive style features.

F. Ablation Study

Now we turn to verify the effects of the composition of our model. We remove the histogram loss, color correction stage, attention module, and skip layers from our model, respectively. Figure 9 shows the ablation experimental results of these four modules. In each group, the left image shows the result without a certain module. In order to demonstrate the results more clearly, we select the most typical image in each ablation experiment. According to Fig. 9, every module plays an important role in our network: the histogram loss significantly improved the definition of the pixels deep inside hole; the attention module better performs in keeping color consistency with similar structure; CCN rectifies obvious color difference in rough result; skip layers help to maintain structural integrity and consistency of color tone.

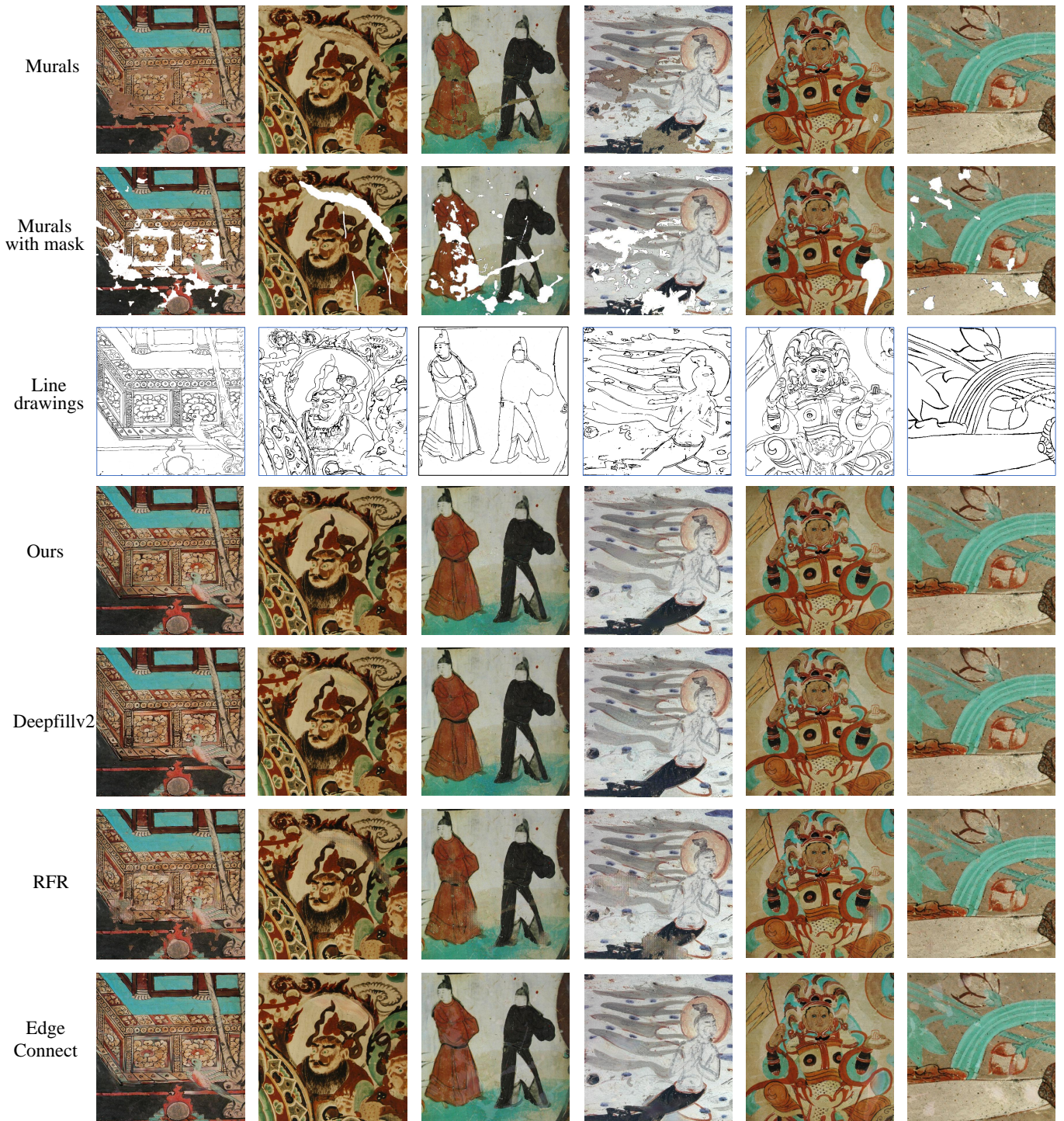


Fig. 7. Experimental results obtained by the proposed method and three comparison methods in repairing real damages of mural images. Deepfillv2, EdgeConnect, and the proposed method take the original mural image, the inpainting mask, and the corresponding line drawing as the input.

V. CONCLUSION

In this work, we proposed a line-drawing-guided progressive inpainting method for repairing mural damages. The pipeline of inpainting was divided into two steps, i.e., structure reconstruction and color correction, which were implemented by a structure reconstruction network (SRN) and a color correction network (CCN), respectively. The line drawing provided a

guarantee for reconstructing the real structure of severely damaged murals. The inpainting strategy separating the structure restoration and color correction alleviated the color bias problem which commonly exists in image inpainting. In addition, a histogram loss was for the first time introduced into image inpainting to improve the repairing quality of large damage holes in the mural image. In the experiments, a dataset

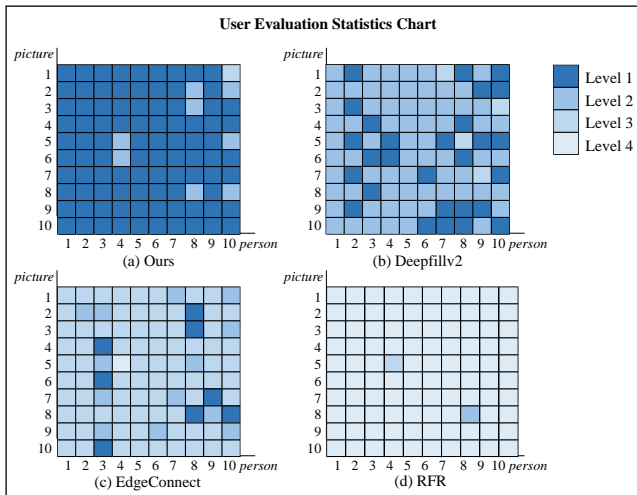


Fig. 8. User evaluation statistics chart. The four statistical graphs from (a) to (d) respectively show the user evaluation results of the four methods. We sorted users' scores from high to low into four levels. The higher the score, the higher the level and the darker the color. Note that the same level is allowed.

for mural image inpainting was constructed on 1,714 mural images which were collected from Dunhuang Mogao Grottoes. The proposed method was evaluated against the current state-of-the-art methods. Qualitative and quantitative results demonstrated the superiority of the proposed method, and the ablation study validated the effectiveness of the designed modules.

REFERENCES

- [1] G. Liu, F. A. Reda, K. J. Shih, T. C. Wang, A. Tao, and B. Catanzaro, "Image inpainting for irregular holes using partial convolutions," *ECCV*, 2018.
- [2] Y. Ren, X. Yu, R. Zhang, T. H. Li, S. Liu, and G. Li, "Structureflow: Image inpainting via structure-aware appearance flow," in *ICCV*, 2019.
- [3] S. Iizuka, E. Simo-Serra, and H. Ishikawa, "Globally and locally consistent image completion," *ACM Transactions on Graphics (TOG)*, vol. 36, no. 4, pp. 1–14, 2017.
- [4] J. Yu, Z. Lin, J. Yang, X. Shen, and T. Huang, "Free-form image inpainting with gated convolution," in *ICCV*, 2019.
- [5] Z. Yi, Q. Tang, S. Azizi, D. Jang, and Z. Xu, "Contextual residual aggregation for ultra high-resolution image inpainting," in *CVPR*, 2020.
- [6] F. Liu, X. Deng, Y.-K. Lai, Y.-J. Liu, C. Ma, and H. Wang, "Sketchgan: Joint sketch completion and recognition with generative adversarial network," in *CVPR*, 2019.
- [7] Z. Liu, P. Luo, X. Wang, and X. Tang, "Deep learning face attributes in the wild," in *ICCV*, 2015.
- [8] B. Zhou, A. Lapedriza, A. Khosla, A. Oliva, and A. Torralba, "Places: A 10 million image database for scene recognition," *PAMI*, vol. 40, no. 6, pp. 1452–1464, 2017.
- [9] C. Doersch, S. Singh, A. Gupta, J. Sivic, and A. Efros, "What makes paris look like paris?" *ACM Transactions on Graphics*, vol. 31, no. 4, 2012.
- [10] K. Nazeri, E. Ng, T. Joseph, F. Z. Qureshi, and M. Ebrahimi, "Edgeconnect: Generative image inpainting with adversarial edge learning," *ICCV Workshops*, 2019.
- [11] J. Yu, Z. Lin, J. Yang, X. Shen, X. Lu, and T. S. Huang, "Generative image inpainting with contextual attention," in *CVPR*, 2018.
- [12] E. Risser, P. Wilmot, and C. Barnes, "Stable and controllable neural texture synthesis and style transfer using histogram losses," *arXiv preprint arXiv:1701.08893*, 2017.
- [13] N. Wang, Y. Zhang, and L. Zhang, "Dynamic selection network for image inpainting," *IEEE Transactions on Image Processing*, vol. 30, pp. 1784–1798, 2021.
- [14] A. Criminisi, P. Pérez, and K. Toyama, "Region filling and object removal by exemplar-based image inpainting," *IEEE Transactions on image processing*, vol. 13, no. 9, pp. 1200–1212, 2004.
- [15] J. Li, F. He, L. Zhang, B. Du, and D. Tao, "Progressive reconstruction of visual structure for image inpainting," in *ICCV*, 2019.
- [16] M. Xie, M. Xia, X. Liu, C. Li, and T.-T. Wong, "Seamless manga inpainting with semantics awareness," *ACM Transactions on Graphics (TOG)*, vol. 40, no. 4, pp. 1–11, 2021.
- [17] H. Liu, B. Jiang, Y. Song, W. Huang, and C. Yang, "Rethinking image inpainting via a mutual encoder-decoder with feature equalizations," in *ECCV*, 2020, pp. 725–741.
- [18] L. Liao, R. Hu, J. Xiao, and Z. Wang, "Edge-aware context encoder for image inpainting," in *2018 IEEE International Conference on Acoustics, Speech and Signal Processing (ICASSP)*. IEEE, 2018, pp. 3156–3160.
- [19] H. Liu, B. Jiang, Y. Xiao, and C. Yang, "Coherent semantic attention for image inpainting," in *ICCV*, 2019, pp. 4170–4179.
- [20] T. Wang, L. Wu, and C. Sun, "A coarse-to-fine approach for dynamic-to-static image translation," *Pattern Recognition*, vol. 123, p. 108373, 2022.
- [21] M.-c. Sagong, Y.-g. Shin, S.-w. Kim, S. Park, and S.-j. Ko, "Pepsi: Fast image inpainting with parallel decoding network," in *CVPR*, 2019.
- [22] N. Wang, S. Ma, J. Li, Y. Zhang, and L. Zhang, "Multistage attention network for image inpainting," *Pattern Recognition*, vol. 106, p. 107448, 2020.
- [23] Y. Zeng, J. Fu, H. Chao, and B. Guo, "Learning pyramid-context encoder network for high-quality image inpainting," in *CVPR*, 2019, pp. 1486–1494.
- [24] J. Qin, H. Bai, and Y. Zhao, "Multi-level augmented inpainting network using spatial similarity," *Pattern Recognition*, vol. 126, p. 108547, 2022.
- [25] X. Ma, X. Zhou, H. Huang, G. Jia, Z. Chai, and X. Wei, "Contrastive attention network with dense field estimation for face completion," *Pattern Recognition*, vol. 124, p. 108465, 2022.
- [26] L. Zhao, Q. Mo, S. Lin, Z. Wang, Z. Zuo, H. Chen, W. Xing, and D. Lu, "Uctgan: Diverse image inpainting based on unsupervised cross-space translation," in *CVPR*, 2020, pp. 5741–5750.
- [27] W. Cai and Z. Wei, "Piigan: generative adversarial networks for pluralistic image inpainting," *IEEE Access*, vol. 8, pp. 48 451–48 463, 2020.
- [28] H. Zhang, Z. Hu, C. Luo, W. Zuo, and M. Wang, "Semantic image inpainting with progressive generative networks," in *Proceedings of the 26th ACM international conference on Multimedia*, 2018, pp. 1939–1947.
- [29] L. Liao, J. Xiao, Z. Wang, C.-W. Lin, and S. Satoh, "Image inpainting guided by coherence priors of semantics and textures," in *CVPR*, 2021, pp. 6539–6548.
- [30] Q. Zou, Y. Cao, Q. Li, C. Huang, and S. Wang, "Chronological classification of ancient paintings using appearance and shape features," *Pattern Recognition Letters*, vol. 49, pp. 146–154, 2014.
- [31] Q. Li, Q. Zou, D. Ma, Q. Wang, and S. Wang, "Dating ancient paintings of mogao grottoes using deeply learnt visual codes," *Science China Information Sciences*, vol. 61, no. 9, pp. 1–14, 2018.
- [32] S. Jaidilert and G. Farooque, "Crack detection and images inpainting method for thai mural painting images," in *2018 IEEE 3rd International Conference on Image, Vision and Computing (ICIVC)*. IEEE, 2018, pp. 143–148.
- [33] Z. Song, W. Xuan, J. Liu, Y. Li, and L. Cao, "Image restoration of dun huang murals based on auto-encoder generative adversarial neural network," in *Advanced Graphic Communication, Printing and Packaging Technology*. Springer, 2020, pp. 186–194.
- [34] I.-M. Ciortan, S. George, and J. Y. Hardeberg, "Colour-balanced edge-guided digital inpainting: Applications on artworks," *Sensors*, vol. 21, no. 6, p. 2091, 2021.
- [35] H. Wang, Q. Li, and Q. Zou, "Inpainting of dunhuang murals by sparsely modeling the texture similarity and structure continuity," *Journal on Computing and Cultural Heritage (JOCCH)*, vol. 12, no. 3, pp. 1–21, 2019.
- [36] N. Wang, W. Wang, W. Hu, A. Fenster, and S. Li, "Damage sensitive and original restoration driven thanka mural inpainting," in *Chinese Conference on Pattern Recognition and Computer Vision (PRCV)*. Springer, 2020, pp. 142–154.
- [37] Q. Guo, X. Li, F. Juefei-Xu, H. Yu, Y. Liu, and S. Wang, "Jpgnet: Joint predictive filtering and generative network for image inpainting," in *Proceedings of the 29th ACM International Conference on Multimedia*, 2021, pp. 386–394.
- [38] M. Chen, X. Zhao, and D. Xu, "Image inpainting for digital dunhuang murals using partial convolutions and sliding window method," in *Journal of Physics: Conference Series*, vol. 1302, 2019, p. 032040.
- [39] N. Wang, W. Wang, W. Hu, A. Fenster, and S. Li, "Thanaka mural inpainting based on multi-scale adaptive partial convolution and stroke-like mask," *IEEE Transactions on Image Processing*, pp. 1057–1149, 2021.

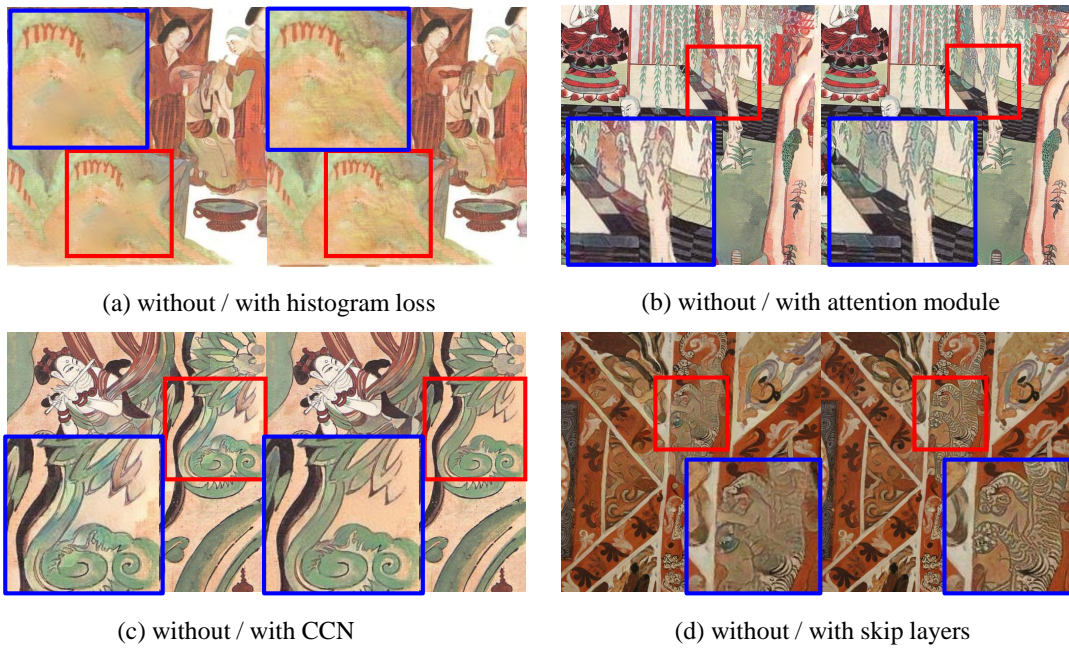


Fig. 9. Four samples (a) to (d) were used to show the ablation experimental results of four modules: histogram loss, attention, CCN, and skip layers, respectively. In each sample, the left image shows the result without a module. In order to demonstrate the results more clearly, we enlarge a part of the image in each ablation experiment.

- [40] V. Badrinarayanan, A. Kendall, and R. Cipolla, “Segnet: A deep convolutional encoder-decoder architecture for image segmentation,” *IEEE transactions on pattern analysis and machine intelligence*, vol. 39, no. 12, pp. 2481–2495, 2017.
- [41] D. Ulyanov, A. Vedaldi, and V. Lempitsky, “Instance normalization: The missing ingredient for fast stylization,” *arXiv preprint arXiv:1607.08022*, 2016.
- [42] P. Isola, J.-Y. Zhu, T. Zhou, and A. A. Efros, “Image-to-image translation with conditional adversarial networks,” in *CVPR*, 2017.
- [43] W. Xiong, J. Yu, Z. Lin, J. Yang, X. Lu, C. Barnes, and J. Luo, “Foreground-aware image inpainting,” in *CVPR*, 2019.
- [44] T. Miyato, T. Kataoka, M. Koyama, and Y. Yoshida, “Spectral normalization for generative adversarial networks,” *arXiv preprint arXiv:1802.05957*, 2018.
- [45] A. L. Maas, A. Y. Hannun, A. Y. Ng *et al.*, “Rectifier nonlinearities improve neural network acoustic models,” in *Proc. icml*, vol. 30, 2013.
- [46] X. Wang, R. Girshick, A. Gupta, and K. He, “Non-local neural networks,” 2018.
- [47] I. Goodfellow, J. Pouget-Abadie, M. Mirza, B. Xu, D. Warde-Farley, S. Ozair, A. Courville, and Y. Bengio, “Generative adversarial nets,” *NIPS*, 2014.
- [48] L. A. Gatys, A. S. Ecker, and M. Bethge, “Image style transfer using convolutional neural networks,” in *CVPR*, 2016.
- [49] F. Luan, S. Paris, E. Shechtman, and K. Bala, “Deep painterly harmonization,” in *Computer graphics forum*, vol. 37, 2018, pp. 95–106.
- [50] X. Soria, E. Riba, and A. Sappa, “Dense extreme inception network: Towards a robust cnn model for edge detection,” in *WACV*, 2020.
- [51] C. Tomasi and R. Manduchi, “Bilateral filtering for gray and color images,” in *ICCV*, 1998.
- [52] J. Li, N. Wang, L. Zhang, B. Du, and D. Tao, “Recurrent feature reasoning for image inpainting,” in *CVPR*, 2020.
- [53] D. P. Kingma and J. Ba, “Adam: A method for stochastic optimization,” *arXiv preprint arXiv:1412.6980*, 2014.
- [54] D. M. Allen, “Mean square error of prediction as a criterion for selecting variables,” *Technometrics*, vol. 13, no. 3, pp. 469–475, 1971.
- [55] Z. Wang, “Image quality assessment : From error visibility to structural similarity,” *IEEE Transactions on Image Processing*, 2004.
- [56] A. Hore and D. Ziou, “Image quality metrics: Psnr vs. ssim,” in *ICPR*, 2010.
- [57] R. Zhang, P. Isola, A. A. Efros, E. Shechtman, and O. Wang, “The unreasonable effectiveness of deep features as a perceptual metric,” in *CVPR*, 2018.
- [58] H. Xiang, Q. Zou, M. A. Nawaz, X. Huang, F. Zhang, and H. Yu, “Deep learning for image inpainting: A survey,” *Pattern Recognition*, vol. 134, p. 109046, 2023.

Luxi Li received the B.E. degree in surveying and mapping from Nanjing Normal University in 2020, and the Master degree in electronic information from Wuhan University in 2022. She was a student member at the Machine Vision and Robotics Laboratory, Wuhan University. She is now pursuing the Ph.D. degree at the United International College of Beijing Normal University - HongKong Baptist University. Her research interests include deep learning and image inpainting.

Qin Zou (M’13-SM’19) received the B.E. degree in information science and the Ph.D. degree in computer vision from Wuhan University, Wuhan, China, in 2004 and 2012, respectively. From 2010 to 2011, he was a visiting Ph.D. student at the Computer Vision Lab, University of South Carolina, Columbia, SC, USA. He is an Associate Professor with the School of Computer Science, Wuhan University. His research activities involve computer vision, pattern recognition, and machine learning. He is currently serving as an Associate Editor for *IEEE Transactions on Intelligent Vehicles*. Dr. Zou was a co-recipient of the National Technology Invention Award of China in 2015.

Fan Zhang received the Ph.D. degree in photogrammetry and remote sensing from Wuhan University, Wuhan, China, in 2009. He is currently an Associate Professor of the State Key Laboratory of Surveying, Mapping, and Remote Sensing Information Engineering, and the Deputy Director of Institute of Aerial and Space Photography, Wuhan University. His research interests include laser point clouds and photogrammetry, machine learning, digital image processing and multi-source image fusion modeling.

Hongkai Yu received the Ph.D. degree in computer science and engineering from University of South Carolina, Columbia, SC, USA, in 2018. He is currently an Assistant Professor in the Department of Electrical Engineering and Computer Science at Cleveland State University, Cleveland, OH, USA. His research interests include computer vision, machine learning, deep learning and intelligent transportation system. He is a member of the IEEE.

Long Chen received the B.Sc. degree in communication engineering and the Ph.D. degree in signal and information processing from Wuhan University, Wuhan, China, in 2007 and in 2013, respectively. From October 2010 to November 2012, he was co-trained PhD Student at National University of Singapore. From 2008 to 2013, he was in charge of environmental perception system for autonomous vehicle SmartV-II with the Intelligent Vehicle Group, Wuhan University. He is a professor with the Institute of Automation, Chinese Academy of Sciences, China. He is currently serving as an associate editor of IEEE Transactions on Intelligent Transportation Systems. His areas of interest include perception system of intelligent vehicle.

Chengfang Song received the Ph.D. degree in computer science and technology from Zhejiang University, Hangzhou, China, in 2007. He was a faculty member with the School of Computer Science, Wuhan University from 2008 to 2021, and is currently an assistant professor with the Reseach Center of GNSS, Wuhan University. His research interests include computer graphics, computational photography, machine learning, and digitalization of cultural heritage.

Xianfeng Huang received the Ph.D. degree in photogrammetry and remote sensing from Wuhan University, Wuhan, China, in 2006. He is a Professor with the State Key Laboratory of Surveying, Mapping, and Remote Sensing Information Engineering, and the Deputy Director of Institute of Aerial and Space Photography, Wuhan University. His research interests include digital image processing, machine learning and digitalization of cultural heritage.

Xiaoguang Wang received the Ph.D. degree in management science and engineering from Wuhan University in 2007. Currently, he is the vice dean and professor of the School of Information Management, Wuhan University. He directs the Philosophy and Social Science Laboratory of the Ministry of Education of Intelligent Computing for Cultural Heritage, and the Digital Humanities Research Center, Wuhan University. He is the executive director of China Audio Video and Digital Publishing Association, the deputy director of the Digital Humanities Special Committee of China Index Society, and the chief expert of major projects of the National Social Science Fund. His research interests include image processing and digitalization of cultural heritage.